

Determination of Gold Nanoparticles Sizes via Surface Plasmon Resonance

Paul K. Ngumbi^{1,2}, Simon W. Mugo¹, James M. Ngaruiya¹

¹Department of Physics, Jomo Kenyatta university of Agriculture and Technology, Kenya

²Department of Physics and Electronics, South Eastern Kenya University, Kenya.

Corresponding author: Paul K. Ngumbi

Abstract: Surface plasmon resonance technique has been highly employed in determination of the sizes of metallic nanoparticles (NPs). Generally, NP size has been viewed as a function of SPR wavelength value only, with every value of this wavelength being associated with one particular size. In this paper, gold NPs (AuNPs) prepared through the citrate reduction method with a variation in the amount of citrate used on gold (III) chloride precursor was studied. Using UV-Vis spectra analysis of the synthesized NPs in colloidal form, SPR absorption band with a wavelength ranging from 518 to 520 nm was detected. At 518 and 519 nm peaks, the recorded average NP size was 12 nm while 520 nm coincided with NPs of diameters 11 and 13 nm. This indicated that small and large AuNPs within the plasmonic size can present similar high resonance. We attribute this observation to the atomic interactions within the NPs solution hence the availability of the high density of the surface (resonance) electrons from the NPs surface atoms.

Key words- Gold NPs, Citrate reduction, Surface plasmon resonance, UV-Vis spectroscopy

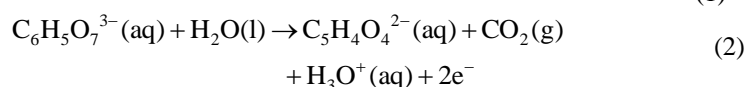
Date of Submission: 22-06-2018

Date of acceptance: 09-07-2018

I. Introduction

The increasing interest in nanotechnology research results from the fact that materials attain new properties at nanoscale, with these properties changing with NPs size or shape [1]. Knowing sizes of the NPs has been crucial to their applications and for noble metal nanomaterials, the strong light absorption known as the localized surface plasmon resonance (LSPR) has been viewed as a promising property in size calculation. This SPR arises from the collective oscillation of the free electrons in the conduction band from one surface of the material nanoparticle to the other as the electrons interact with electromagnetic radiations [2]. Such electrons oscillate at a frequency capable of absorbing visible light, hence giving rise to the vivid characteristic color of NPs. For colloidal gold NPs, their wine red color is thus due to their SPR [3, 4] features, which depends on the size, shape, and concentration of the NPs [5-7].

Recently, much of activity has been in the synthesis and characterization of NPs with different sizes and shapes. For small and uniform particles, chemical routines are more suitable and probably most common procedure for preparation of metal NPs, based on the theory of nucleation and particle growth [8, 9]. In preparation of uniform AuNPs, one of the most common procedures is the chemical reduction of the Au(III) aqueous solution by citrate ions near the boiling point (~100 °C) to produce AuNPs in the form of a stable solution. The Au(III) ions are usually added to water in the form of hydrogen tetrachloroaurate ($\text{HAuCl}_4 \cdot 3\text{H}_2\text{O}$). Citrate ions ($\text{C}_6\text{H}_5\text{O}_7^{3-}$), which are mostly oxidized to acetone dicarboxylate ions ($\text{C}_5\text{H}_4\text{O}_4^{2-}$) in the process, act as a two-electron reducing agent. This process is as described by equations 1 and 2, with the citrate ions serving also as a capping agent and a pH mediator [10] that determine the final size and distribution of the NPs.



In this work, colloidal gold NPs samples were prepared through HAuCl_4 reduction by varying the amount of citrate used. From the UV-Vis absorption spectra of the solutions, NPs sizes were determined based on the LSPR wavelength peaks values for each sample. A plot of LSPR peak value against the NP size was generated. Within the plasmonic range, the LSPR peak value can be associated to different NP sizes.

II. Materials and Methods

Hydrogen tetrachloroaurate (III) trihydrate (ACS reagent, ≥ 49.0 Au basis, $\text{HAuCl}_4 \cdot 3\text{H}_2\text{O}$, $\text{MW}=393.83$ g/mol), trisodium citrate dihydrate tribasic ($\text{Na}_3\text{C}_6\text{H}_5\text{O}_7$, $\text{MW}=294.1$ g/mol, 99%), Hydrochloric acid and Nitric acid were sourced from sigma Aldrich, and used as received. Deionized, ultra-filtered water (DIUF H_2O) with resistivity $\sim 18\text{M}\Omega\text{-cm}$ was used for final cleaning and as a solvent in this work. Prior to use, the glassware was first cleaned in hot soapy water and soaked in freshly prepared aqua regia (3:1HCl/ HNO_3 v/v) for 6 hours, rinsed in DIUF H_2O , and finally oven-drying.

A solution of 0.01% w/v $\text{HAuCl}_4 \cdot 3\text{H}_2\text{O}$ was prepared by dissolving 0.0500 g of the gold salt in 50 mL of the DIUF H_2O , then diluting it to a volume of 500 mL. A standard solution of $\sim 0.1\%$ w/v Na_3Ctr was prepared by dissolving 0.5705 g of the solute to form 50 mL with the DIUF H_2O . A 50 mL volume of the precursor solution was transferred into a 100 mL flask and heated on a hot plate under vigorous magnetic stirring [11] until boiling (at $\sim 98^\circ\text{C}$). Seven aliquots of the citrate solution were taken in steps of 0.05 mL from 0.85 to 1.15 mL and each introduced into an independent flask with the boiling solution under rapid stirring. It was allowed to boil further (~ 6 minutes) attaining a final wine red colour after which heating was stopped and the solution cooled to room temperature under maintaining the stirring.

The presence of AuNPs in the resulting solution was established based on characteristic colour which involves light absorption within the visible spectrum, and Tyndall effect resulting from scattering of light upon interacting with the particles in the solution. The NPs size determination was done through UV-Vis spectroscopy, a technique based on absorption of light by molecules within the UV-Vis region [12]. In this study, UV-Vis spectra of the solutions were recorded on a Shimadzu UV-1800 spectrophotometer (Shimadzu UV-spectrophotometer) in a standard $1\text{ cm} \times 1\text{ cm} \times 3.5\text{ cm}$ quartz cuvette at a resolution of 1 nm from 300 to 800 nm.

III. Results

Size analysis for gold nanoparticles prepared by varying the volume of Na_3Ctr solution is presented. The prepared AuNPs solution had a wine red colour which resulted as a complementary colour while the other portion of the spectrum is absorbed by the NPs, mainly within the SPR wavelength. The solution also experienced Tyndall scattering effect under a 632.8 nm laser beam (Figure 1, inset). This effect is due to the light scattering by the colloidal AuNPs (< 20 nm) as they interact with the laser beam, which is an indication that the size of the prepared NPs is capable of absorbing light within the plasmonic frequency range.

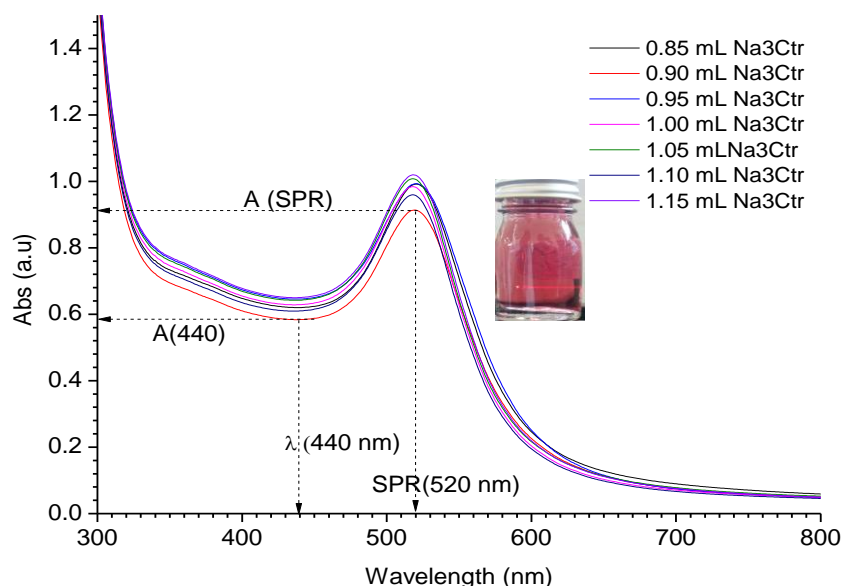


Figure 1: UV-Vis Spectra for the synthesized gold NPs at different volumes of the Na_3Ctr showing the absorbance values $A(\text{SPR})$ and $A(440)$ as used in calculating NP sizes. (Inset): Wine red AuNPs solution showing Tyndall effect on laser illumination

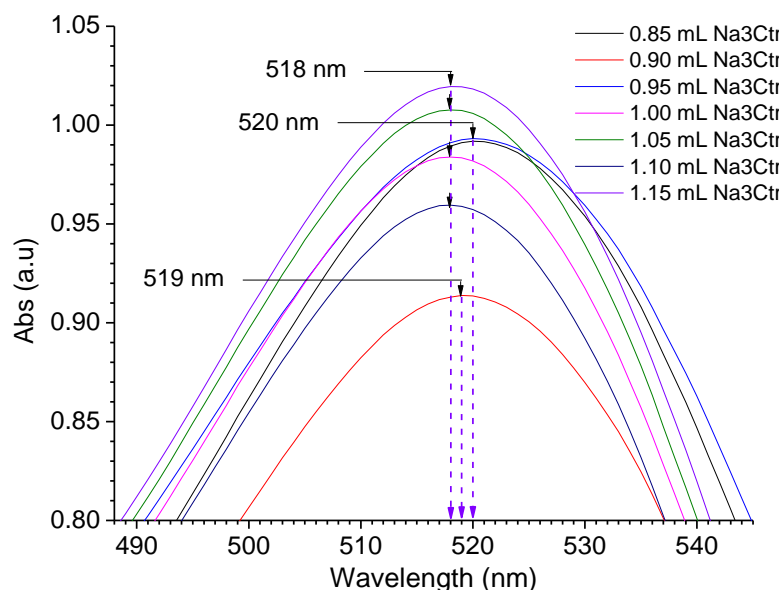


Figure 2: Absorption spectra for the synthesized AuNPs showing the positions of SPR band peaks

Confirmation of the visual observations made, and determination of the sizes of the prepared AuNPs was done based on the UV–Vis spectrophotometer absorption data, recorded in the wavelength range of 300 – 800 nm at room temperature. Absorption spectra for the seven NP sample solutions (Figure 1) indicated that the SPR band range between 518 and 520 nm (Figure 2) from the different volumes of Na₃Citr (Figure 3). This gives a further support to the production of AuNPs as previous reported [13].

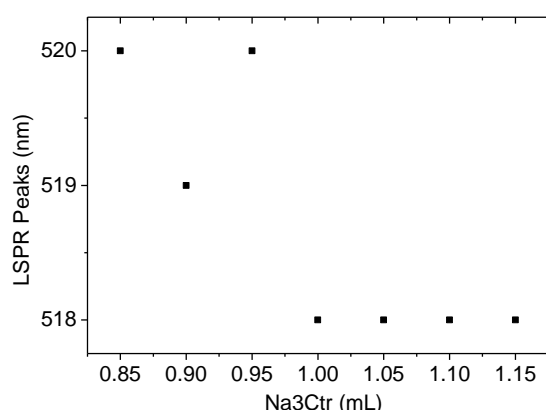


Figure 3: Variation of SPR peaks with the volume of citrate used in AuNPs synthesis

IV. Discussion

The observed absorption band wavelength range is a characteristic of AuNPs and results from the SPR which gives rise to their distinctive red colour. For small NPs (<20 nm), interband transitions have a strong effect on the position of the SPR [14] and for AuNPs, this transition “pushes” the resonance to 2.4 eV (~530 nm), compared to bulk gold which is 10 - 15 eV (~510 nm). The position of SPR bands has been previously used in the determination of particle size [15], where the size (D) of AuNPs can be calculated from equation (3);

$$D = \exp \left(B_1 \frac{A_{SPR}}{A_{450}} - B_2 \right) \quad (3)$$

Here, B_1 and B_2 parameters experimentally determined as 3.00 and 2.20 respectively with the ratio A_{SPR} / A_{450} being particularly suitable in calculating the particle diameter (nm), where A_{SPR} is the absorbance at SPR while A_{450} is the lowest absorbance close to the peak, occurring at 450 nm. Applying equation 3 to our data, the lowest absorbance generally occurs at 440 nm (Figure 1) hence the ratio A_{SPR} / A_{440} was adopted.

The dependence of the ratio A_{SPR} / A_{440} on the logarithm of the particle diameter within our narrow size range indicates that the logarithmic size of the particles [15] is within the range 2.4 to 2.6 which translates to NPs of size from ~11 to 14 nm representing a case of poly-dispersity. Using the SPR band wavelengths, NPs sizes (D) has been previously calculated as in equation 4 [16];

$$D = 2.99 \lambda_{SPR} + 1539 \quad (4)$$

where the SPR wavelength, λ_{SPR} is the only variable. From our data, λ_{SPR} was compared to sizes generated from reported studies (Figure 4) based on equation 4.

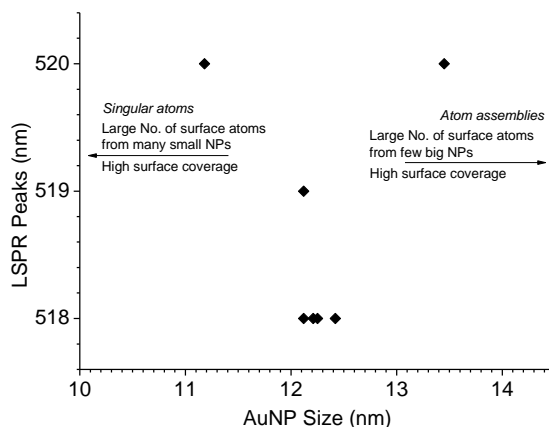


Figure 4: Variation in SPR peaks with AuNPs sizes where different SPR peaks are associated with a particular NP sizes and vice versa within the range 10 - 15 nm

Analysis of the relationship between our NPs sizes and LSPR peak wavelengths (Figure 4) reveals that, for AuNPs within the size range of 10-15 nm, the LSPR peaks ranges from 518 to 520 nm. We herein observed that, in the synthesis of AuNPs, a critical size of ~12 nm is attained as shown above, and corresponded to a wavelength of 518 nm. As the sizes of the NPs reduce, the LSPR value is reported as 520 nm, similar to when the NPs size increases to ~15 nm. This above observation can be attributed to the effect of atomic surface coverage which affects the surface electrons responsible for the SPR in AuNPs

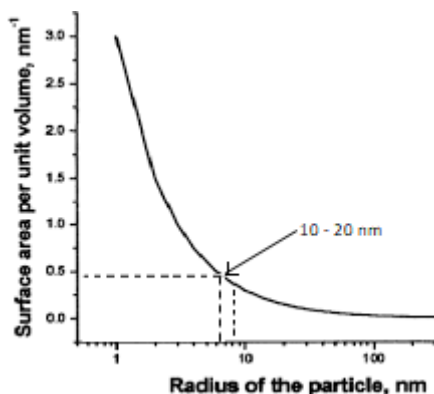


Figure 5: Surface-to-volume ratios of nanocomposite spheres as a function of nanoparticle size [17]

Considering a given volume of solution containing AuNPs within the plasmonic region, the NPs interactions and variations in the inter-particle distances results to numerous small NPs (<12 nm). These NPs exist as singular atoms or agglomerates while the fewer larger NPs behave like atomic assemblies occupying a similar volume. Nanoparticles have great fraction of their atoms on their surface which leads to a high surface area to volume ratio (Figure 5). This ratio is associated with surface energy that makes "dangling bonds" at the surface. Atoms at the surface are under-coordinated, and because breaking bonds costs energy, surface atoms always have higher energy than atoms in the bulk. This energy can be characterized in terms of the SPR and used to analyze the size of NPs. The limit of 10 to 15 nm in diameter of AuNPs forms a critical size since the surface area to volume ratio decay approaches its minimal value. Within this limit, NPs can exhibit SPR slightly below or above the 520 nm, which is regarded as the optimal SPR peak for AuNPs.

V. Conclusion

From our colloidal AuNPs UV-Vis spectrophotometry, we show that NPs of diameter 10 to 15 nm occurs within the plasmonic size range and coincide with any SPR peak value from 518 to 520 nm. The average AuNPs size attained based on the citrate reduction method in this study was ~12 nm and coincided with SPR at 518 nm.

References

- [1]. Barberio, M., Antici, P., 2017. In situ study of nucleation and aggregation phases for nanoparticles grown by laser-driven methods. *Sci. Rep.* 7, 41372. <https://doi.org/10.1038/srep41372>
- [2]. Long, N.N., Vu, L.V., Kiem, C.D., Doanh, S.C., Nguyet, C.T., Hang, P.T., Thien, N.D., Quynh, L.M., 2009. Synthesis and optical properties of colloidal gold nanoparticles. *J. Phys. Conf. Ser.* 187, 012026. <https://doi.org/10.1088/1742-6596/187/1/012026>
- [3]. He, X., Lu, H., 2014. Graphene-supported tunable extraordinary transmission. *Nanotechnology* 25, 325201. <https://doi.org/10.1088/0957-4484/25/32/325201>
- [4]. Mie, G., 1908. Beiträge zur Optik trüber Medien, speziell kolloidaler Metallösungen. *Ann. Phys.* 330, 377–445. <https://doi.org/10.1002/andp.19083300302>
- [5]. Amendola, V., Meneghetti, M., 2009. Size Evaluation of Gold Nanoparticles by UV–vis Spectroscopy. *J. Phys. Chem. C* 113, 4277–4285. <https://doi.org/10.1021/jp8082425>
- [6]. Jain, P.K., Lee, K.S., El-Sayed, I.H., El-Sayed, M.A., 2006. Calculated Absorption and Scattering Properties of Gold Nanoparticles of Different Size, Shape, and Composition: Applications in Biological Imaging and Biomedicine. *J. Phys. Chem. B* 110, 7238–7248. <https://doi.org/10.1021/jp057170o>
- [7]. Kelly, K.L., Coronado, E., Zhao, L.L., Schatz, G.C., 2003. The Optical Properties of Metal Nanoparticles: The Influence of Size, Shape, and Dielectric Environment. *J. Phys. Chem. B* 107, 668–677. <https://doi.org/10.1021/jp026731y>
- [8]. Polte, J., 2015. Fundamental growth principles of colloidal metal nanoparticles – a new perspective. *CrystEngComm* 17, 6809–6830. <https://doi.org/10.1039/C5CE01014D>
- [9]. Becker, R., Doring, W., 1935. Kinetic treatment of the nucleation in supersaturated vapors. *Ann Phys* 24, 719–752.
- [10]. Ji, X., Song, X., Li, J., Bai, Y., Yang, W., Peng, X., 2007. Size Control of Gold Nanocrystals in Citrate Reduction: The Third Role of Citrate. *J. Am. Chem. Soc.* 129, 13939–13948. <https://doi.org/10.1021/ja074447k>
- [11]. Merza, K.S., Al-Attabi, H.D., Abbas, Z.M., Yusr, H.A., 2012. Comparative Study on Methods for Preparation of Gold Nanoparticles. *Green Sustain. Chem.* 02, 26–28. <https://doi.org/10.4236/gsc.2012.21005>
- [12]. Faust, C.B., 1992. *Modern chemical techniques: background reading for students and chemistry teachers.* Royal Society of Chemistry, London].
- [13]. Sunatkari, A.L., Talwatkar, S.S., Tamgadge, Y.S., Muley, G.G., 2016. Synthesis, characterization and properties of L-arginine-passivated silver nanocolloids. p. 020663. <https://doi.org/10.1063/1.4946714>
- [14]. Patungwasa, W., Hodak, J.H., 2008. pH tunable morphology of the gold nanoparticles produced by citrate reduction. *Mater. Chem. Phys.* 108, 45–54. <https://doi.org/10.1016/j.matchemphys.2007.09.001>
- [15]. Haiss, W., Thanh, N.T.K., Aveyard, J., Fernig, D.G., 2007. Determination of Size and Concentration of Gold Nanoparticles from UV–Vis Spectra. *Anal. Chem.* 79, 4215–4221. <https://doi.org/10.1021/ac0702084>
- [16]. Ghosh, D., Chattopadhyay, N., 2013. Gold Nanoparticles: Acceptors for Efficient Energy Transfer from the Photoexcited Fluorophores. *Opt. Photonics J.* 03, 18–26. <https://doi.org/10.4236/opj.2013.31004>
- [17]. Keith Nelson, J. (2007). Overview of nanodielectrics: Insulating materials of the future (pp. 229–235). *IEEE*. <https://doi.org/10.1109/EEIC.2007.4562626>

IOSR Journal of Applied Chemistry (IOSR-JAC) is UGC approved Journal with Sl. No. 4031, Journal no. 44190.

Paul K. Ngumbi "Determination of Gold Nanoparticles Sizes via Surface Plasmon Resonance." *IOSR Journal of Applied Chemistry (IOSR-JAC)* 11.7 (2018): 25-29.